ACS APPLIED BIO MATERIALS

www.acsabm.org Article

Gradient and Dynamic Hydrogel Materials to Probe Dynamics in Cancer Stem Cell Phenotypes

Junmin Lee,* Amr A. Abdeen, Yanfen Li, Shamalee Goonetilleke, and Kristopher A. Kilian*

Cite This: https://dx.doi.org/10.1021/acsabm.0c01263 Read Online

ACCESS | Metrics & More | Article Recommendations | Supporting Information

ABSTRACT: The microenvironment of tumors shows high variability in stiffness compared to normal tissues, suggesting that spatiotemporal changes in mechanics play a role in development and progression. Here, we employ microengineered hydrogels with static, dynamic (magnetic field-mediated stiffening and softening), or gradient matrix elasticity to investigate the influence of matrix mechanics in modulating the stem cell-like phenotype in melanoma and breast cancer cells. Using immunofluorescence staining of molecular markers associated with a cancer stem cell (CSC) state, we show that a subtle increase in local stiffness promotes the CSC phenotype, while different mechanical properties in static or dynamic hydrogels—without gradient profiles of mechanical properties—have a negligible influence on phenotype switching toward a CSC state. Inhibition of integrins and downstream effectors of mechanotransduction reveals that distinct signaling pathways play a role in regulating the dynamic CSC state in melanoma and breast cancer cells. Our findings demonstrate how cancer cells respond to the local stiffness gradients with dynamic plasticity during progression.

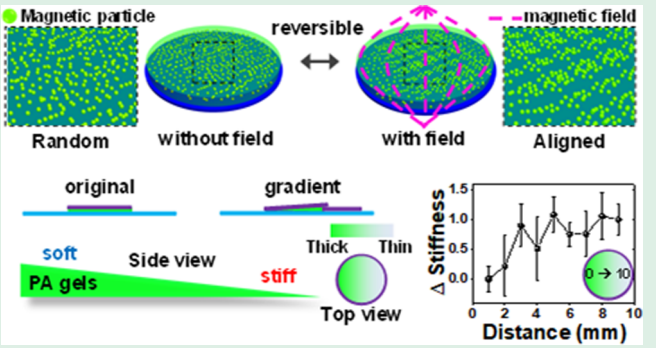

KEYWORDS: *cancer stem cells, melanoma, breast cancer, matrix stiffness, dynamic stiffening, stiffness gradient, mechanotransduction, cancer cell plasticity*

1. INTRODUCTION

There is compelling evidence in numerous cancers that the cells responsible for recurrence and metastasis have the characteristics of stem cells,[1] that is, the ability to self-renew and differentiate into all the cells of the tumor mass. These studies have led to the "cancer stem cell (CSC)" model that explains the phenotypic and functional heterogeneity observed across the tumor volume.[2] An alternative model is that of "clonal evolution" which holds that mutations across the tumor cell population give rise to subsets of cells with competitive advantage through natural selection processes.[3] In reality, these models are not mutually exclusive; that is, a stem-like cancer cell may undergo clonal evolution to generate a more metastatic phenotype.[4] This is best represented by the variability in tumorigenic properties across different cancers. For instance, in breast cancer, there is significant evidence for a distinct CSC population that is resistant to many chemotherapeutics and shows high metastatic potential and tumorigenic properties.[5] Breast cancer cells that do not express stem cell markers have been shown to lack tumorigenicity thus supporting the CSC model. In contrast, while tumorigenic melanoma stem cells have been identified, normal melanoma cells have been shown to change into a tumorigenic, CSC-like state and form new tumors in support of a clonal evolution model.[6] There are clear differences in the dominant mechanisms from which tumorigenicity arises in cancers, and reconciling these differences in the context of the microenvironment and the role of the extracellular matrix (ECM) is essential to modeling pathogenesis in a laboratory.

A diverse array of microenvironmental factors is known to regulate cell activities.[7−9] In particular, accumulated evidence over the last several decades has shown that the ECM where cells adhere plays a crucial role in cell fate decision through biochemical and physical factors including adhesive ligands,[10,11] matrix elasticity,[12] and topography.[13] Among these factors, mechanical stiffness of the ECM is known to have a major influence on a range of cellular processes such as migration,[14,15] proliferation,[16] and differentiation.[17] For example, lineage specification of mesenchymal stem cells is regulated by matrix stiffness itself or through the combined influence of multiple factors together.[18,19] In addition, recent studies suggest that the matrix elasticity of the ECM is also a key modulator of cancer cell behaviors such as invasiveness,[20]

Received: September 29, 2020
Accepted: December 4, 2020

the induction of epithelial to mesenchymal transition (EMT),[21] progression,[22] and the regulation of a small subset of cells with the characteristic of stem cells, the so-called CSCs.[23] However, most of these findings employ overly simplistic and static biomaterials which present a fixed microenvironment to cells. In contrast, cells in vivo reside within a complex and dynamic microenvironment where stiffness is invariably heterogeneous and dynamic.

Cancer cells possess widespread mechanisms of migration and invasion,[24] and the ECM plays an important role in invasive properties which is a key step in tumor infiltration and metastasis.[25] Studies have shown that ECM rigidity strongly influences the phenotypes and migration and invasion characteristics of tumors.[26−28] For example, a tumor-associated ECM has been shown to be stiffer than the surrounding tissues for breast cancer cells,[29] and alterations of ECM elastic modulus can affect the migration and proliferation rate of brain tumor cells.[30] Moreover, recent evidence has revealed that tumor cells show plasticity of their malignant phenotypes in response to microenvironmental factors.[27,31,32] For instance, breast CSC gene expression could be promoted with stiff tissues as well as low oxygen tension through modulation of integrin-linked kinase and the PI3K/Akt pathway.[27] However, a recent report showed that ECM rigidity could not significantly affect proliferation, differentiation potential, or expression of tumor-initiating cell markers of glioblastoma.[33] These divergent studies suggest that "cell state-invasion" relationships are more complicated than originally appreciated, thereby requiring model systems that match this complexity.

It is well appreciated that cells exert less tension on softer substrates. Stiffness gradients, imposed onto cells during ECM stiffening, plays an important role in regulating morphology,[34] apoptosis,[35] migration,[36] mechanosensing,[37] and differentiation.[38,39] For example, cells cultured on gels with stiffness gradients show an increase in the spreading area and cytoskeleton organization with increasing matrix stiffness.[34] In addition, it was reported that cancer cells cultured in substrates with stiffness gradients infiltrate more into soft regions (∼0.3 kPa) compared to those penetrating into stiffer regions (∼1.2 or 6 kPa); however, those cultured on stiffer regions show reduced apoptotic susceptibility to chemotherapeutic treatment.[35] Although it has been investigated that local tissue mechanics provide important signals to the behaviors of cancer cells, the role of heterogeneous microenvironments with gradient rigidity in the potential transformation of cancer cells into malignant phenotypes is currently unknown.

Recently, we showed that the invasive character of melanoma cells is highly dependent on topological cues ranging from the peripheral curvature to variations in surface energy at the growth interface, which promotes EMT and reprogramming to a CSC state, yet matrix elasticity did not display significant influences on CSC marker expression.[40−42] One possibility for this result could be the simple, static, and homogeneous stiffness used to investigate the relation between matrix elasticity and CSC markers. Therefore, we hypothesized that using complex microenvironments such as dynamic or gradient stiffness to recapitulate the complex tissue structure and function may allow us to precisely understand how cancer cell behaviors are regulated by dynamic and changing matrix properties. Here, we employ engineered hydrogel substrates that mimic variations in mechanical stiffness of microenvironments in vivo (static vs dynamic vs gradient), and explore how changing mechanics regulates the CSC-like state in melanoma and breast cancer.

2. MATERIALS AND METHODS

2.1. Materials. All materials were obtained from Sigma unless otherwise noted. Glass coverslips (18 mm circular) and tissue culture plastic were purchased from Fisher Scientific. Cell culture media and reagents [fetal bovine serum (FBS) and penicillin/streptomycin (P/S)] were purchased from Thermo Fisher. Rabbit anti-ABCB5 (NBP1-77687) and anti-CD133 (MB S462020) were purchased from Novus and Biorbyt, respectively. Mouse anti-CD271 (AM1842a), anti-CD44 (AB6124), and anti-$\alpha5\beta1$ (MAB1969) were purchased from Abgent, Abcam, and Millipore, respectively. Y-27632, FR180204 (ERK inhibitor), and SB202190 (p38 inhibitor) were purchased from Calbiochem. Alexa Fluor 488-conjugated anti-rabbit (AB150077) and 647-conjugated anti-mouse (AB150115) IgG antibodies were purchased from Abcam. Alexa 555-phalloidin (A34055) and 4,6-diamidino-2-phenylindole (DAPI, D3571) were purchased from Invitrogen.

2.2. Surface Preparation. For static polyacrylamide (PA) hydrogels, we employed the previously reported protocol.[43] Briefly, PA gels with 1, 10, and 100 kPa stiffness were made on a glass coverslip (18 mm) by mixtures of varying amounts of acrylamide and bis-acrylamide. 0.1% ammonium persulfate and tetramethylenediamine were used for initiating the reaction. Coverslips were activated with 3-aminopropyltriethoxysilane for 3 min and glutaraldehyde for 30 min, and 20 μL of the mixture (gel solution) was sandwiched between the activated coverslip and a hydrophobically treated (RainX) glass slide. After polymerization with an appropriate time for each stiffness condition, the gel-coated coverslips were gently detached and treated with hydrazine hydrate 55% by rocking for 2 h to modify the surface chemistry. After hydrazine treatment, 5% glacial acetic acid was added for 1 h to rinse the hydrazine, and then distilled water was added at least for 1 h to remove the glacial acetic acid. Nonpatterned polydimethylsiloxane (Polysciences) stamps were produced on the flat surfaces of plasticware. Sodium periodate (∼3.5 mg/mL) was added to fibronectin (25 μg/mL) in 1× phosphate-buffered saline (PBS) for at least 45 min to generate free aldehydes on the glycoproteins. The oxidized protein solution was pipetted onto nonpatterned stamps for 30 min and dried with air. The protein residue on the stamps was transferred to the gel surface via microcontact printing; free aldehydes on proteins could be chemically conjugated to reactive hydrazine groups on the gel surface.

For gradient PA gels, we used the same procedure as making static PA gels except for using a spacer and the amount of gel solution to make gels. Specifically, to fabricate gradient gels, 40 μ of the mixture (gel solution) was sandwiched between the hydrophobically treated glass slide, and the treated coverslip and a spacer (another cleaned coverslip, 0.17 mm) were located at one side of the treated coverslip to create a thickness gradient.

For dynamic PA gels, we used the previously reported protocol.[44] Briefly, it is based on the method for fabricating static PA gels, but the only difference is to add carbonyl iron (CI) particles (grade EW, QED Technologies) in the mixture of gel solution. CI particles were washed with distilled water at least four times before use. The desired mixture of these particles by volume was prepared in the gel solution (0.5 kPa as a desired stiffness). 20 μ of the mixture (gel solution + CI particles) was sandwiched between the activated coverslip and a hydrophobically treated glass slide for polymerization. Stiffness was reversibly changed from 0.5 kPa (without magnetic field, 0 T) to 10 kPa (with magnetic field, ∼0.2 T).

2.3. Mechanical Characterization. For the static and gradient gels, the Young's moduli of the matrices were obtained based on contact force measurements using atomic force microscopy (AFM, Asylum Research) as previously reported.[43] Before the measurement, AFM tips (Bruker) were calibrated in the air and then in PBS. Then, all measurements (∼10 measurements at different spots) were performed in PBS for the static and gradient gels across at least three samples. A Hertz model using IGOR Pro software (Wave-

https://dx.doi.org/10.1021/acsabm.0c01263
ACS Appl. Bio Mater. XXXX, XXX, XXX−XXX

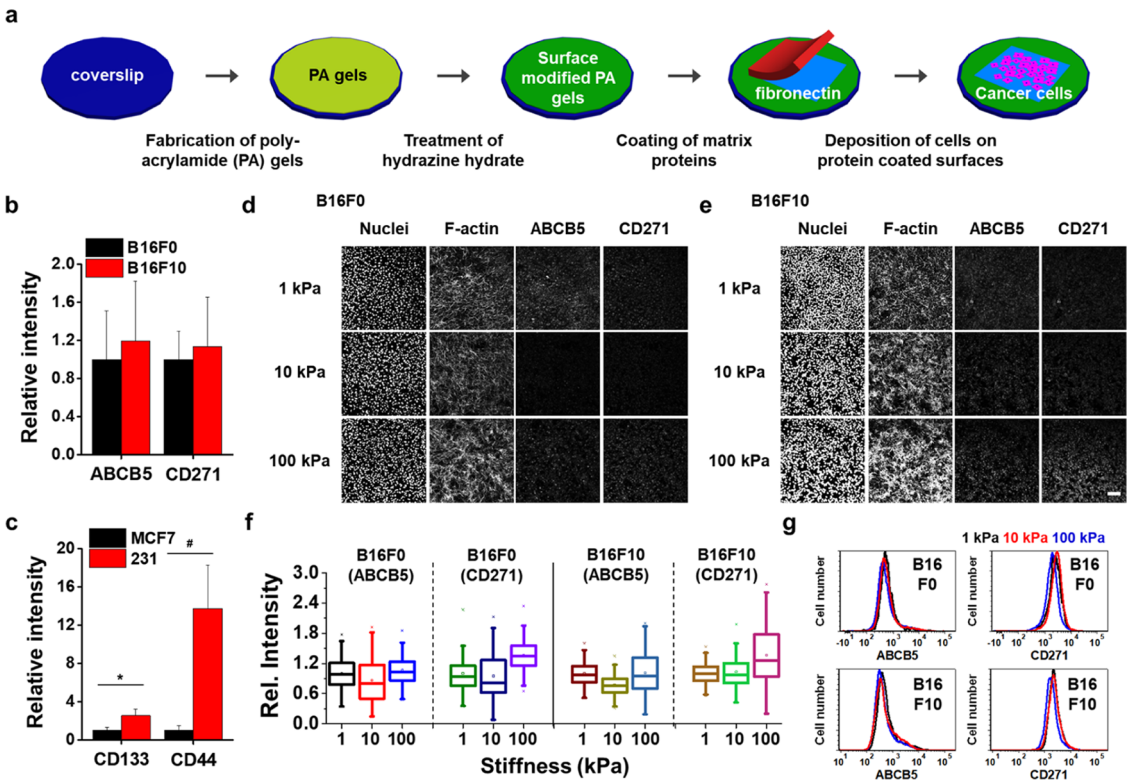

Figure 1. Cells cultured on static and homogeneous substrates with different stiffness show no significant change for CSC marker expression. (a) Schematic showing the process used to culture cells on fibronectin-coated PA gels (nonpatterned). Quantitation of CSC marker expression for (b) B16F0 and B16F10 cells (ABCB5 and CD271) and (c) human MCF7 and MDA-MB-231 cells cultured on 10 kPa gels for 5 days. Representative confocal microscope images of (d) B16F0 and (e) B16F10 cells stained for nuclei, F-actin, ABCB5, and CD271 cultured on substrates with three different stiffness for 5 days. Expression of CSC markers using (f) immunofluorescence and (g) flow cytometry for B16F0 and B16F10 cells cultured on static substrates with different matrix rigidity (1, 10, and 100 kPa). Scale bar: 100 μm. Error bar: SD. $^{*}P < 0.05$, $^{\#}P < 0.01$ ($N = 3$).

Metrics) was employed to fit the obtained data, and the tip geometry was assumed as a cone architecture to acquire the Young's modulus values.

For the dynamic gels, elastic moduli were obtained based on dynamic shear measurements using a rotational rheometer (combined-motor-transducer, DHR-3, TA Instruments) with a magneto-rheology (MR) setup (magnetic fields from −1 to +1 T) as previously reported.[44] Briefly, measurements of samples (disk shape with 1 mm-thickness and 20 mm-diameter) were performed with a nonmagnetic parallel plate fixture (20 mm-diameter): an electromagnetic coil applying magnetic field lines orthogonal to the plate surface as well as a hall probe under the plate leading to real time measurement of the external field strength throughout the tests at a constant temperature (37 °C), oscillation (1 rad/s), and shear strain amplitude (1% in the linear viscoelastic regime) with a closed-loop control fluid circulator through the bottom MR fixture.

2.4. Cell Source and Culture. Cancer cell lines B16F0 and B16F10 (murine melanoma) and MCF7 and MDA-MB-231 (human breast) were obtained from the American Type Culture Collection (ATCC) and cultured according to the protocols recommended. For cell culture, media (Dulbecco's modified Eagle's medium supplemented with 10% FBS and 1% P/S) was changed every three to four days and cells were passaged at nearly 95% confluence using 0.25% trypsin.

2.5. Immunochemistry. Cells were fixed after 5 days in culture with 4% paraformaldehyde (PFA) for 20 min and permeabilized with 0.1% Triton X-100 (Fisher) in PBS for 30 min. To block the cells, 1% bovine serum albumin (BSA) was used for 15 min and primary antibodies in 1% BSA overnight at 4 °C with rabbit anti-ABCB5 (1:500) and mouse anti-CD271 (1:250) for melanoma cells and rabbit anti-CD133 (1:500) and mouse anti-CD44 (1:250) for breast cancer cells. Secondary antibody labeling was performed with DAPI (1:2500), Alexa 488-conjugated anti-rabbit (1:200), Alexa 555-phalloidin (1:200), and 647-conjugated anti-mouse (1:200) in 2% goat serum, with 1% BSA in PBS for 20 min in a humid chamber (5% CO_2 & 37 °C). Immunofluorescence microscopy was conducted using an LSM (Carl Zeiss) which is a laser point scanning confocal microscope with a single pinhole.

2.6. Cell Labeling and Flow Cytometry. Melanoma (B16F0 and B16F10) and breast cancer (MCF7 and 231) cells cultured for five days on static gels with 1, 10, and 100 kPa stiffness (12 identical substrates) were trypsinized and broken down into a single cell suspension. Cells were fixed with 4% PFA for 20 min. To permeabilize cells, 0.1% Triton X-100 in PBS was used for 30 min. Cells were blocked in 1% BSA for 15 min and labeled with primary antibodies (the same condition in the procedure of immunochemistry) in 1% BSA overnight at 4 °C. Next, secondary antibodies [Alexa 488-conjugated anti-rabbit (1:200) and 647-conjugated anti-mouse (1:200)] in 2% goat serum and 1% BSA in PBS were applied for 20 min in a humid chamber (5% CO_2 & 37 °C). After every step, cells were washed three times with PBS. A BD LSRFortessa flow cytometry analyzer was employed to measure immunofluorescence intensity of single cells, and cells stained without primary antibodies were employed as negative controls to set the baseline.

2.7. Inhibition Assays. Inhibitors and blocking antibodies were added to cell cultured media at the following concentration before and after cell seeding and with each media change: 1 μg/mL anti-$\alpha5\beta1$ (MAB1969), 2 mM Y-27632 (Calbiochem), 6 mM p38 (Calbiochem: SB202190) and ERK (Calbiochem: FR180204), and 0.1 μg/mL noggin (SB-505124, Sigma). Isotype controls were used during optimization of blocking procedures for several previous studies[13,19,40,41] and are not included in this manuscript.

2.8. Microscopy Data Analysis. ImageJ software was employed to analyze immunofluorescence images. Single cells were manually

https://dx.doi.org/10.1021/acsabm.0c01263
ACS Appl. Bio Mater. XXXX, XXX, XXX−XXX

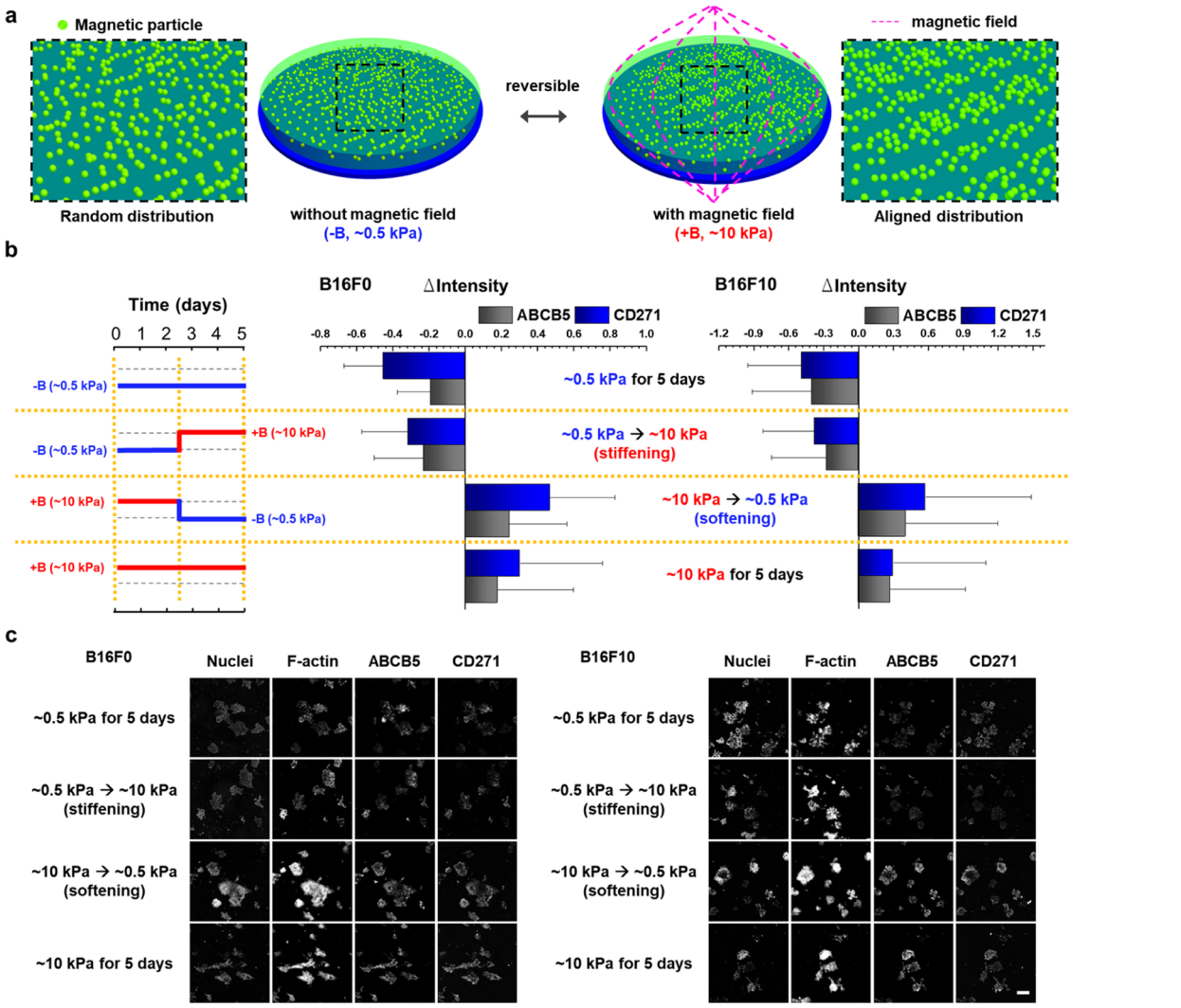

Figure 2. Dynamic stiffening regulates the expression of CSC markers for melanoma cells. (a) Schematic illustrating stiffening PA hydrogels incorporating CI particles by applying magnetic fields to align the particles. (b) Magnetization profile for dynamic stiffening for 5 days in culture and the percent change of ABCB5 and CD271 expression relative to average of all samples at day 5 in melanoma cells. (c) Representative images of nuclei, F-actin, ABCB5, and CD271. Scale bar: 100 μm. Error bar: SD (N = 3).

segmented using DAPI and F-actin images, and the segmented single cells (over 100 cells for each condition) were used for measuring intensities of different markers; multiple cells overlapped each other were excluded in the analysis. The mean intensities of the markers were used to obtain the average intensity values and their standard deviation (SD). The relative intensity of fluorescence was determined by comparing each intensity value to one of the values among conditions.

2.9. Statistical Analysis. Data was obtained from at least three independent experiments, and error bars represent SD. For statistical analysis, we used two-tailed P-values from Student's t-test for comparing two groups and analysis of variance with Tukey HSD post-hoc testing for comparisons of more than two groups. Differences were considered significant at $P < 0.05$.

3. RESULTS

3.1. Influence of Homogeneous Stiffness on CSC Marker Expression. We prepared microengineered hydrogels (static: ~1, 10, 100 kPa, dynamic: ~0.5 ↔ ~10 kPa reversibly, and gradient: ~10 kPa) and employed soft lithography to transfer matrix proteins onto the surface of the hydrazine-modified hydrogels with flat surfaces without a structure (nonpatterned). To explore the effects of matrix rigidity on CSC marker expression, we selected different malignant tumors of the murine B16 melanoma cell lines (B16F0: less metastatic and B16F10: more metastatic) and human breast cancer cell lines (MCF7: non-metastatic and 231: metastatic) and employed putative CSC molecular markers (ABCB5 and CD271 for B16 melanoma and CD44 and CD133 for breast cancers). We first measured these markers in the cells with a different degree of malignancy after 5 days in culture on fibronectin-conjugated hydrogels (10 kPa) (Figure 1a). More metastatic B16F10 cells expressed slightly higher tumorigenic molecular markers than B16F0 cells, while metastatic 231 cells showed significantly higher expression levels of CSC markers compared to non-metastatic MCF7 (Figure 1b,c). To investigate the role of the stiffness of the underlying matrix, these cells were cultured on the substrates with different elasticity (~1, 10, and 100 kPa) where stiffness is homogeneous. Expression of CSC markers (immunofluorescence and flow cytometry) seemed not dependent on the matrix rigidity regardless of the cell type or metastatic potency (Figures 1d–g and S1), which corresponds to previous studies.[33,40]

https://dx.doi.org/10.1021/acsabm.0c01263
ACS Appl. Bio Mater. XXXX, XXX, XXX−XXX

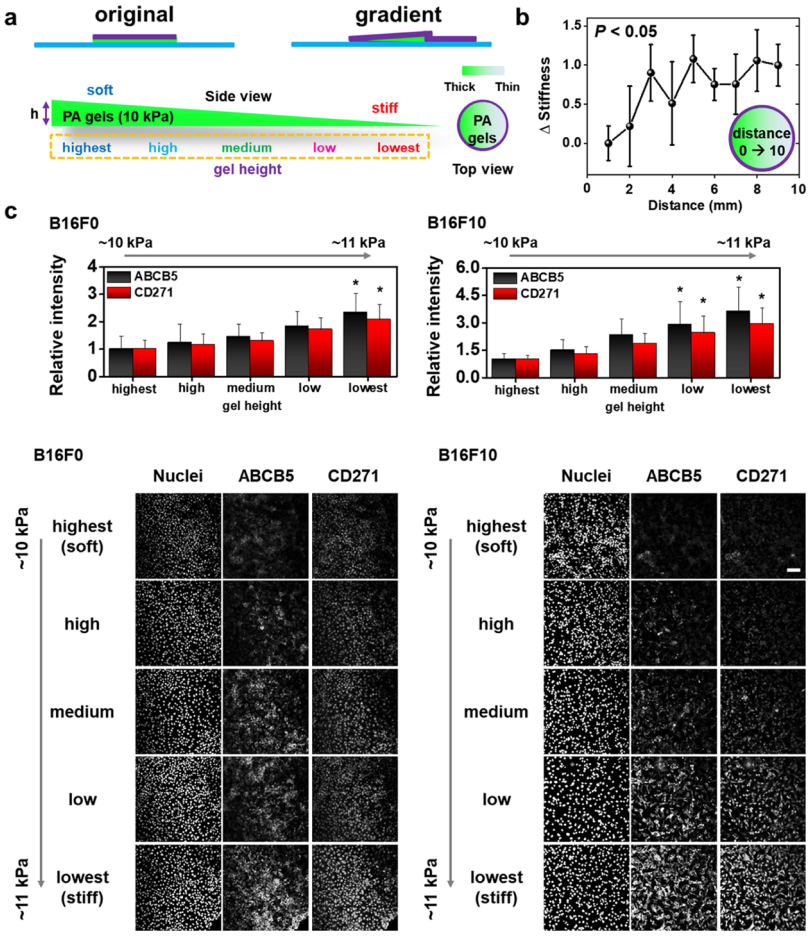

Figure 3. Stiffness gradient hydrogel formation and its effects on CSC marker expression of melanoma cells. (a) Formation of gradient gels using a spacer and force−deflection curves of the gels. (b) Measured Young's modulus of gradient hydrogels (0: thickest and 10: thinnest). Error bar: standard error of the mean. (c) Relative ABCB5 and CD271 marker intensity of melanoma cells cultured on stiffness gradient gels and their representative images on different regions of the gels. Scale bar: 100 μm. Error bar: SD. *$P < 0.05$ ($N = 3$).

3.2. Influence of Dynamic Stiffness on the CSC Phenotype. Because the microenvironment in vivo is complex and dynamic and thus stiffness of the matrix is heterogeneous, we first employed magnetoactive hydrogels with dynamically tunable stiffness by a magnetic field from 0.5 (w/o field) to 10 kPa (w/field) reversibly where temporal modulation of the matrix stiffness is possible (Figure 2a).[44] Cells were seeded on fibronectin-conjugated gels containing magnetic particles with or without a magnetic field, and the stiffness was changed at day 2.5. We then imaged and measured CSC marker expression for each cell line at 5 days. To highlight different levels of CSC marker expression between each condition [(i) ∼0.5 kPa for 5 days, (ii) ∼0.5 kPa for 2.5 days and ∼10 kPa for 2.5 additional days (matrix stiffening), (iii) ∼10 kPa for 2.5 days and then ∼0.5 kPa for 2.5 additional days (matrix softening), and (iv) ∼10 kPa for 5 days], the average value of all cells measured at day 5 across the conditions was first obtained. Then, CSC expression levels of single cells in each condition were subtracted by the average value of the entire groups. Finally, the average intensity values for each condition were obtained to clearly display deviation of CSC marker expression.[44] Analysis of expression of those CSC markers indicates that initial stiffening might play a dominant role in CSC states especially for B16 melanoma cancers relative to stiffening (∼0.5 to ∼10 kPa) or softening (∼10 to ∼0.5 kPa) of the matrices even though the effects are not statistically significant (Figure 2b,c). For instance, B16 cells initially cultured on stiff substrates showed higher levels of CSC marker expression compared to those initially cultured on soft substrates (Figure 2b), while breast cancer cells express similar levels of CSC markers irrespective of initial stiffness (Figure S2). Surprisingly, stiffening or softening during 5 days in culture did not exert any influence on CSC marker expression for both cancer cell lines.

3.3. Influence of Stiffness Gradients on the Expression of CSC Markers. To further investigate the role of stiffness on CSC states, we next fabricated gels by creating a continuous gradient on a gel layer. It is possible for cells to locally sense a different degree of stiffness in the gels because although homogeneous gels were used, the different thickness between the gels and a coverslip leads to a subtle difference in stiffness felt by the cells for the overall substrates (Figure 3a). To verify homogeneous bioconjugation of matrix proteins, we first transferred an Alexa-555-conjugated fibrinogen onto the hydrazine-treated surface of gradient gels. Immunofluorescence analysis of the conjugated gels shows no significant difference from the fluorescence intensity across all the regions unrelatedly of gel rigidity (Figure S3). Interestingly, unlike cells cultured on simply static or dynamic gels with different matrix rigidity showing no difference in CSC marker expression, those cultured for 5 days on the gradient gels expressed significantly different levels of CSC markers (both

https://dx.doi.org/10.1021/acsabm.0c01263
ACS Appl. Bio Mater. XXXX, XXX, XXX−XXX

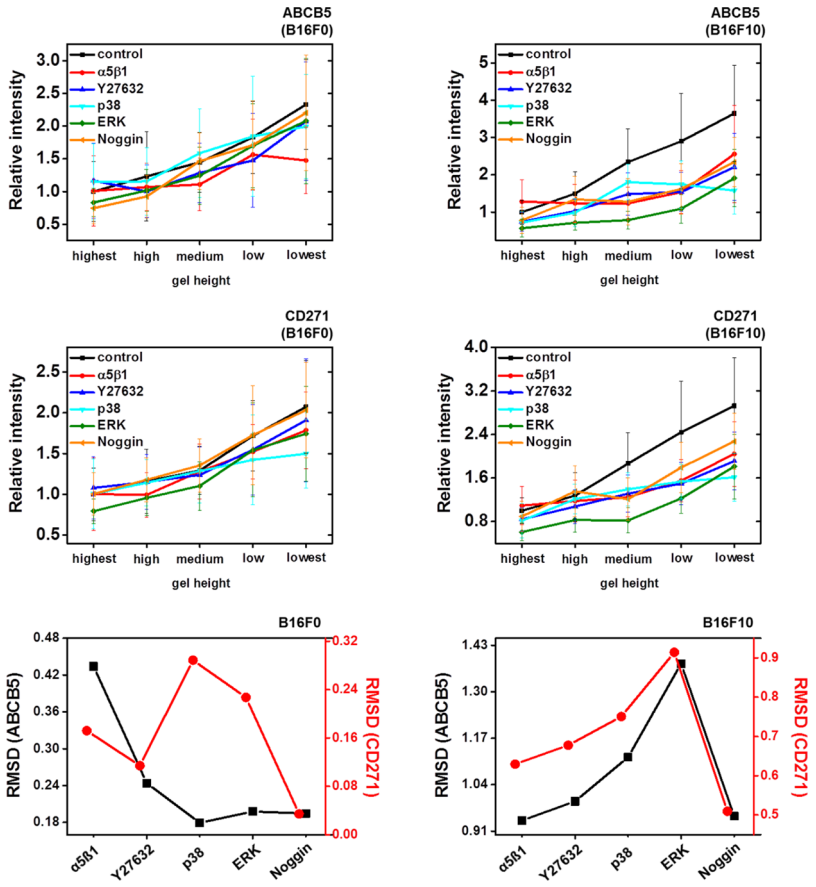

Figure 4. Inhibition of integrins and downstream effectors influence CSC marker expression. Expression of CSC markers (ABCB5 and CD271) for melanoma cells cultured on gradient gels with or without inhibitors and RMSD of the results. Error bar: SD (N = 3).

B16 melanoma and breast cancer cell lines) depending on the local stiffness, a maximum at the lowest gel height (the stiffest, ~11 kPa) and a minimum at the highest gel height (the softest, ~10 kPa) (Figures 3b and S4) (intensity ratio: stiffness/softest, for B16F0: ~2.3-fold (ABCB5) and ~2.1-fold (CD271), for B16F10: ~3.6-fold (ABCB5) and ~2.9-fold (CD271), for MCF7: ~1.8-fold (CD133) and ~2.6-fold (CD44), for 231: ~1.9-fold (CD133 and CD44)). This suggests that cancer cells in response to the local changes in stiffness could be activated into a CSC-like state. However, we noticed that the mechanical properties in Figure 3b were likely saturated after ~3 mm, suggesting that stiffness may be roughly constant beyond a 3 mm distance from the highest thickness. We acknowledge that there are some other possible factors including cell migration which might also play a role in regulating CSC states during culture. Nevertheless, because it is obvious that cell migration on the gradient gels could be affected by the local matrix stiffness which might be interdependent, our claim that the gradient hydrogels could regulate the CSC states by modulating local mechanical properties of matrices is still viable.

To further verify the influence of stiffness gradient on the expression of CSC markers, we also measured these markers in B16F0 melanoma cells cultured for 1−5 days on nonpatterned gradient substrates and their cell numbers in different regions (Figure S5). Analysis of the CSC marker expression showed that cells adhered onto the stiffer region express higher levels of these markers at day 1 and increase these levels compared to those on softer regions (intensity ratio: stiffness/softest, for ABCB5 day 1: ~1.3-fold, day 2: ~1.4-fold, day 3: ~2.0-fold, day 4: ~2.4-fold, day 5: ~2.7-fold and for CD271 day 1: ~1.3-fold, day 2: ~1.3-fold, day 3: ~1.4-fold, day 4: ~1.4-fold, day 5: ~1.7-fold), indicating that it is likely due to the activation of CSC states for cells which respond at early time points by stiffness gradient that exists on the substrates and increases with culture day. The average number of cells per region was similar within 3 days in culture; however, cells cultured in softer regions grew faster than those cultured in stiffer regions, which corresponds to the previous reports revealing a low proliferation rate for the CSC phenotype. Taken together, our results reveal a clear influence of heterogeneous stiffness using stiffness gradient on promoting the expression of CSC markers when compared to influences of homogeneous rigidity based on the static or dynamic substrates. However, we acknowledge that some variability in cell behaviors like migration or cytokine secretion across the gradient substrates may affect the CSC phenotype outcome.

3.4. Role of Stiffness Gradients in Revealing a CSC Phenotype. We previously revealed that generation of the CSC phenotype with enhanced metastasis and tumorigenicity was achieved not only by tumor periphery activation through integrin $\alpha5\beta1$ adhesion, mitogen activated protein kinase (MAPK), and signal transducer and activator of transcription activity[40] but also by matrix composition via bone morphogenetic protein (BMP) signaling pathways.[45] In the current study, we have shown that subtle changes in matrix rigidity will influence CSC marker expression on gradient gels. To clarify signal transduction pathways that are involved in

https://dx.doi.org/10.1021/acsabm.0c01263
ACS Appl. Bio Mater. XXXX, XXX, XXX−XXX

linking matrix stiffness recognition to the CSC phenotype, we treated cells cultured on gradient gels with integrin-blocking antibodies for $\alpha5\beta1$, the Rho-associated kinase inhibitor Y-27632, mechanotransduction-related MAPK inhibitors (p38 and ERK), and the BMP inhibitor (noggin). Both B16 melanoma and breast cancer cells were cultured in non-patterned gradient substrates with or without 1 μg/mL anti-$\alpha5\beta1$, 2 mM Y-27632, 6 mM p38 and ERK, and 0.1 μg/mL noggin for 5 days. We employed representative CSC markers for both B16 melanoma (ABCB5 and CD271) and breast (CD44 and CD133) cancers to investigate the effects of inhibitors on the activation of CSCs via local stiffness gradient (Figures 4 and S6). Root mean square deviation (RMSD) analysis reveals that the expression of two different CSC markers for each cell line does not show similar trends in response to the inhibition except for B16F10 cells. For B16F0 cells, the expression of ABCB5 shows the highest RMSD when cells are blocked by $\alpha5\beta1$, while p38 inhibition is the most effective inhibition for the expression of CD271. However, B16F10 cells treated with ERK inhibitors show the highest RMSD for both CSC markers. For breast cancers, the highest RMSD for the CD44 expression is shown when treated with p38 (MCF7) or blocked by $\alpha5\beta1$ (231), while the expression of CD133 is more likely to be affected by Y-27632 (MCF7) or noggin (231).

4. DISCUSSION

In this study, we cultured cancer cells on three different substrates (static, dynamic, and gradient) to investigate the relationship between the condition of matrix rigidity and CSC marker expression for melanoma (B16F0 and B16F10) and breast cancer (MCF7 & 231) cells of varying metastatic potential. We could vary matrix stiffness dynamically by using magnetoactive hydrogels (0.5−10 kPa) and employed gradient gels which contain heterogeneous stiffness based on the different thickness of gels on a glass coverslip. We found that cancer cells cultured for 5 days on the stiffer regions of gradient substrates express higher levels of CSC markers regardless of cell type and malignancy. However, dynamic changes in matrix rigidity between 0.5 and 10 kPa do not play an important role in CSC states, which is in line with the results for cells cultured on the substrates with different matrix stiffness (1, 10, and 100 kPa) showing no significant difference of the CSC marker expression.

The influence of matrix rigidity of static gels on CSC marker expression that we observe is consistent with the report by Kumar and co-workers showing that glioblastomas cultured on different matrix stiffness display no major difference in proliferation, differentiation potential, or expression of tumor-initiating cell markers.[33] In addition, we have shown that the expression of CSC markers of melanoma cells is dependent not on matrix rigidity but on topological cues including the curvature and perimeter/area.[40] However, interestingly, it is in contrast to previous studies that a stiffened ECM promotes the invasion of mammary epithelial cells in vitro and malignant conversion and metastasis of mammary tissues in vivo.[29] For example, Wang and co-workers demonstrated the regulation of tumor cell differentiation and proliferation by the mechanical properties of substrates; selected growth of tumorigenic melanoma cells can be promoted by soft fibrin gels.[32] Another report by Nelson and co-workers showed the CSC gene expression of breast cancer cells is affected by matrix stiffness (soft: ∼0.13 & stiff: ∼4.02 kPa) as well as hypoxic conditions.[27] This may be due to the fact that very soft substrates for cancer cells lead to a decrease in focal adhesion, contractility, and mechanosignaling with specific integrin, preventing transformation into malignant phenotype and tumor progression. Unlike these findings, we observed no notable shift toward CSC phenotypes for cancer cells cultured on the static hydrogels, regardless of their stiffness (∼1, 10, and 100 kPa), as well as on the magnetoactive hydrogels with dynamically tunable stiffness (∼0.5 ↔ 10 kPa without or with magnetic fields) but with significant regulation of CSC states for those cultured on the gradient hydrogels (∼10−11 kPa). Our findings suggest that mechanical properties in homogeneous substrates may not lead to changes in CSC phenotypes, while subtle gradients of matrix stiffness may play a role in local regulation of CSC states. However, we acknowledge that further studies are necessary to cross-compare between different hydrogel systems and cancer cell types to uncover general biophysical phenomena (especially associated with homogeneous/gradient matrix stiffness) underlying CSC states within the native tumor microenvironment.

An increase in protein abundance with their reorganization and post-translational modifications leads to ECM stiffening, and one of the important features of tumor microenvironments is the existence of local physical and chemical gradients that influence the tumor phenotype.[46] Studies have shown that tissue stiffness increases as a function of tumor stage and the invasive front of tumors is the region of the stiffest.[47] Moreover, invasion is promoted by these local micro-environmental gradients, which eventually leads to cancer progression and metastasis.[48] It has been shown that invasion for breast and squamous cells cultured on a stiffened ECM is promoted by integrin focal adhesions with the improvement of growth factor and G protein-coupled receptor signaling activating various signaling pathways such as Rho GTPases, Wnt, MAPK, and PI3K.[28,49]

To aid in understanding the role that stiffness gradient plays in regulating the CSC phenotype, we performed inhibition studies using the target mechanotransduction pathways which have been implicated in promoting CSC states. After culturing on gradient gels with or without the inhibitors, we see that multiple signals in cancer cells contribute to the change into a CSC phenotype in response to the heterogeneous matrix rigidity. For B16F0 cells, inhibition of $\alpha5\beta1$ or p38 shows a large decrease in CSC markers (ABCB5 or CD271, respectively), while inhibition of ERK signaling leads to the highest decrease in the expression of both CSC markers for B16F10 cells. Although B16F0 cells are the less metastatic origin of B16F10 cells, the two cell lines show different responses to perceiving a mechanical gradient. Previously, we showed that tumor periphery activation of melanoma cells by perimeter geometry is mediated by signaling pathways through $\alpha5\beta1$ adhesion and MAPK (p38 and ERK).[40] This result is in line with our data for melanoma cells cultured on stiffness gradients, suggesting that the observed activation may converge on similar pathways apparent in geometric regulation. For breast cancer cells, different signaling pathways from melanoma cells in response to the local stiffness gradients were observed. Inhibition of Y27632 for MCF7 and noggin for 231 gives rise to the highest decrease in CD133 expression, while inhibition of p38 for MCF7 and $\alpha5\beta1$ for 231 leads to the largest decline in CD44 expression. It was reported that cancer migration and metastasis were regulated by Rho/ROCK

https://dx.doi.org/10.1021/acsabm.0c01263
ACS Appl. Bio Mater. XXXX, XXX, XXX−XXX

signaling via focal adhesion dynamics[50] and p38 MAPK lies downstream of Rho-kinase (ROCK) for breast cancer cells,[51] indicating that focal adhesion propagated through both ROCK and p38 MAPK signaling may activate CSC-like states for MCF7 in response to local stiffness gradients. Modulation of integrin-related signaling promoted CSC activation for 231 cells when cultured on stiff substrates.[27] In addition, BMPs are known to belong to the transforming growth factor β superfamily and play an important role in breast cancer initiation, proliferation, apoptosis, and the process of metastasis.[52] For instance, breast cancer cells maintained their mesenchymal phenotype with the BMP pathway which promotes more migratory and invasive phenotypes.[53,54] However, MCF7 cells were like CSC phenotypes with reduced BMP7 expression.[55] These results indicate that distinct molecular pathways regulate CSC states for two different breast cancer cell lines, MCF7 and 231, in response to local stiffness gradients. However, we acknowledge that further studies will be required to investigate the detailed signaling pathways regulating CSC phenotypes on the gradient gels including measuring ERK substrate phosphorylation in different regions and conducting independent inhibition of multiple proteins in the given pathways. Nevertheless, in this study, we provided some clues that different signaling pathways may be associated with the promotion of CSC phenotypes on the gradient gels in various cancer types as well as different expression levels of CSC markers could be affected by distinct signaling pathways.

5. CONCLUSIONS

In this work, we explored how variable matrix mechanics influence the CSC phenotype using microengineered hydrogels with static, dynamic, or gradient matrix elasticity. Cells cultured on static and homogeneous gels show no stiffness dependence in the expression of markers associated with CSCs. Dynamic regulation of matrix stiffness also shows no appreciable difference in CSC marker expression. In contrast, cancer cells cultured on substrates that present local stiffness gradients to mimic heterogeneous mechanics in vivo show a significant increase. These results demonstrate how CSC phenotypes in adherent cancer cells are best controlled through subtle changes in the heterogeneous mechanics of the substrate, suggesting that gradient mechanics in tissues give rise to shifts in cancer cell plasticity. The observed sensitivity to heterogenous mechanics is akin to observations in vivo where gradient microenvironments often foster invasive signaling and underscores the importance of presenting cells in vitro with substrates that reflect native microenvironments. We expect that this platform will be broadly applicable across other cancer types and their behaviors that are affected by the physical environment and assist in vitro efforts aimed at unravelling the myriad signals responsible for cancer cell plasticity.

■ ASSOCIATED CONTENT

Supporting Information

The Supporting Information is available free of charge at https://pubs.acs.org/doi/10.1021/acsabm.0c01263.

Expression of CSC markers (immunofluorescence and flow cytometry) for breast cancer cells; CSC marker expression for breast cancer cells on dynamic gels; relative intensity of FITC fibrinogen patterned on gradient gels; CSC marker expression for breast cancer cells on stiffness gradient gels; relative cell number and CSC marker expression for B16F0 cells on stiffness gradient gels; and inhibitor effects on CSC marker expression for breast cancer cells on stiffness gradient gels (PDF)

■ AUTHOR INFORMATION

Corresponding Authors

Junmin Lee − *Department of Materials Science and Engineering, University of Illinois at Urbana-Champaign, Urbana, Illinois 61801, United States; Terasaki Institute for Biomedical Innovation, Los Angeles, California 90064, United States;* orcid.org/0000-0002-4414-7130; Email: jlee@terasaki.org

Kristopher A. Kilian − *Department of Materials Science and Engineering and Department of Bioengineering, University of Illinois at Urbana-Champaign, Urbana, Illinois 61801, United States; School of Chemistry, School of Materials Science and Engineering, Australian Centre for NanoMedicine, University of New South Wales, Sydney, New South Wales 2052, Australia;* orcid.org/0000-0002-8963-9796; Email: k.kilian@unsw.edu.au

Authors

Amr A. Abdeen − *Department of Materials Science and Engineering, University of Illinois at Urbana-Champaign, Urbana, Illinois 61801, United States*

Yanfen Li − *Department of Bioengineering, University of Illinois at Urbana-Champaign, Urbana, Illinois 61801, United States*

Shamalee Goonetilleke − *Department of Materials Science and Engineering, University of Illinois at Urbana-Champaign, Urbana, Illinois 61801, United States*

Complete contact information is available at: https://pubs.acs.org/10.1021/acsabm.0c01263

Author Contributions

The manuscript was written through contributions of all authors. All authors have approved the final version of the manuscript.

Notes

The authors declare no competing financial interest.

■ ACKNOWLEDGMENTS

This research was supported by funding from the National Science Foundation Grant # 1454616 CAR and the National Health and Medical Research Council Grant # APP1185021. We thank the Beckman Institute ITG facilities, Institute of Genomic Biology Imaging facilities, and Micro and Nanotechnology Laboratory facilities.

■ REFERENCES

(1) Schatton, T.; Frank, M. H. Cancer Stem Cells and Human Malignant Melanoma. *Pigm. Cell Melanoma Res.* **2008**, *21*, 39−55.
(2) Dalerba, P.; Cho, R. W.; Clarke, M. F. Cancer Stem Cells: Models and Concepts. *Annu. Rev. Med.* **2007**, *58*, 267−284.
(3) Magee, J. A.; Piskounova, E.; Morrison, S. J. Cancer Stem Cells: Impact, Heterogeneity, and Uncertainty. *Cancer Cell* **2012**, *21*, 283−296.
(4) Meacham, C. E.; Morrison, S. J. Tumour Heterogeneity and Cancer Cell Plasticity. *Nature* **2013**, *501*, 328−337.

(5) Yu, Y.; Ramena, G.; Elble, R. C. The Role of Cancer Stem Cells in Relapse of Solid Tumors. *Front. Biosci.* **2012**, *E4*, 1528−1541.
(6) Lee, N.; Barthel, S. R.; Schatton, T. Melanoma Stem Cells and Metastasis: Mimicking Hematopoietic Cell Trafficking? *Lab. Invest.* **2014**, *94*, 13−30.
(7) Lutolf, M. P.; Hubbell, J. A. Synthetic Biomaterials as Instructive Extracellular Microenvironments for Morphogenesis in Tissue Engineering. *Nat. Biotechnol.* **2005**, *23*, 47−55.
(8) Murphy, W. L.; Mcdevitt, T. C.; Engler, A. J. Materials as Stem Cell Regulators. *Nat. Mater.* **2014**, *13*, 547−557.
(9) Abdeen, A. A.; Lee, J.; Kilian, K. A. Capturing Extracellular Matrix Properties in Vitro: Microengineering Materials to Decipher Cell and Tissue Level Processes. *Exp. Biol. Med.* **2016**, *241*, 930−938.
(10) Kilian, K. A.; Mrksich, M. Directing Stem Cell Fate by Controlling the Affinity and Density of Ligand-Receptor Interactions at the Biomaterials Interface. *Angew. Chem., Int. Ed. Engl.* **2012**, *51*, 4891−4895.
(11) Lee, J.; Abdeen, A. A.; Zhang, D.; Kilian, K. A. Directing Stem Cell Fate on Hydrogel Substrates by Controlling Cell Geometry, Matrix Mechanics and Adhesion Ligand Composition. *Biomaterials* **2013**, *34*, 8140−8148.
(12) Engler, A. J.; Sen, S.; Sweeney, H. L.; Discher, D. E. Matrix Elasticity Directs Stem Cell Lineage Specification. *Cell* **2006**, *126*, 677−689.
(13) Kilian, K. A.; Bugarija, B.; Lahn, B. T.; Mrksich, M. Geometric Cues for Directing the Differentiation of Mesenchymal Stem Cells. *Proc. Natl. Acad. Sci. U.S.A.* **2010**, *107*, 4872−4877.
(14) Saez, A.; Ghibaudo, M.; Buguin, A.; Silberzan, P.; Ladoux, B. Rigidity-Driven Growth and Migration of Epithelial Cells on Microstructured Anisotropic Substrates. *Proc. Natl. Acad. Sci. U.S.A.* **2007**, *104*, 8281−8286.
(15) Park, J.; Kim, D.-H.; Kim, H.-N.; Wang, C. J.; Kwak, M. K.; Hur, E.; Suh, K.-Y.; An, S. S.; Levchenko, A. Directed Migration of Cancer Cells Guided by the Graded Texture of the Underlying Matrix. *Nat. Mater.* **2016**, *15*, 792−801.
(16) Skardal, A.; Mack, D.; Atala, A.; Soker, S. Substrate Elasticity Controls Cell Proliferation, Surface Marker Expression and Motile Phenotype in Amniotic Fluid-Derived Stem Cells. *J. Mech. Behav. Biomed. Mater.* **2013**, *17*, 307−316.
(17) Lee, J.; Abdeen, A. A.; Kilian, K. A. Rewiring Mesenchymal Stem Cell Lineage Specification by Switching the Biophysical Microenvironment. *Sci. Rep.* **2014**, *4*, 5188.
(18) Frith, J. E.; Mills, R. J.; Hudson, J. E.; Cooper-White, J. J. Tailored Integrin-Extracellular Matrix Interactions to Direct Human Mesenchymal Stem Cell Differentiation. *Stem Cells Dev.* **2012**, *21*, 2442−2456.
(19) Lee, J.; Abdeen, A. A.; Tang, X.; Saif, T. A.; Kilian, K. A. Biomaterials Geometric Guidance of Integrin Mediated Traction Stress during Stem Cell Differentiation. *Biomaterials* **2015**, *69*, 174−183.
(20) Sil, H.; Sen, T.; Chatterjee, A. Fibronectin-Integrin ($\alpha5\beta1$) Modulates Migration and Invasion of Murine Melanoma Cell Line B16F10 by Involving MMP-9. *Oncol. Res.* **2011**, *19*, 335−348.
(21) Gomez, E. W.; Chen, Q. K.; Gjorevski, N.; Nelson, C. M. Tissue Geometry Patterns Epithelial-Mesenchymal Transition via Intercellular Mechanotransduction. *J. Cell. Biochem.* **2010**, *110*, 44−51.
(22) Lu, P.; Weaver, V. M.; Werb, Z. The Extracellular Matrix: A Dynamic Niche in Cancer Progression. *J. Cell Biol.* **2012**, *196*, 395−406.
(23) Allen, M.; Louise Jones, J. Jekyll and Hyde: The Role of the Microenvironment on the Progression of Cancer. *J. Pathol.* **2011**, *223*, 163−177.
(24) Friedl, P.; Gilmour, D. Collective Cell Migration in Morphogenesis, Regeneration and Cancer. *Nat. Rev. Mol. Cell Biol.* **2009**, *10*, 445−457.
(25) Barney, L. E.; Dandley, E. C.; Jansen, L. E.; Reich, N. G.; Mercurio, A. M.; Peyton, S. R. A Cell-ECM Screening Method to Predict Breast Cancer Metastasis. *Integr. Biol.* **2015**, *7*, 198−212.
(26) Lin, H.-H.; Lin, H.-K.; Lin, I.-H.; Chiou, Y.-W.; Chen, H.-W.; Liu, C.-Y.; Harn, H. I.-C.; Chiu, W.-T.; Wang, Y.-K.; Shen, M.-R.; Tang, M.-J. Mechanical Phenotype of Cancer Cells: Cell Softening and Loss of Stiffness Sensing. *Oncotarget* **2015**, *6*, 20946−20958.
(27) Pang, M.-F.; Siedlik, M. J.; Han, S.; Stallings-Mann, M.; Radisky, D. C.; Nelson, C. M. Tissue Stiffness and Hypoxia Modulate the Integrin-Linked Kinase Ilk to Control Breast Cancer Stem-like Cells. *Cancer Res.* **2016**, *76*, 5277−5287.
(28) Paszek, M. J.; Zahir, N.; Johnson, K. R.; Lakins, J. N.; Rozenberg, G. I.; Gefen, A.; Reinhart-King, C. A.; Margulies, S. S.; Dembo, M.; Boettiger, D.; Hammer, D. A.; Weaver, V. M. Tensional Homeostasis and the Malignant Phenotype. *Cancer Cell* **2005**, *8*, 241−254.
(29) Boyd, N. F.; Rommens, J. M.; Vogt, K.; Lee, V.; Hopper, J. L.; Yaffe, M. J.; Paterson, A. D. Mammographic Breast Density as an Intermediate Phenotype for Breast Cancer. *Lancet Oncol.* **2005**, *6*, 798−808.
(30) Ulrich, T. A.; De Juan Pardo, E. M.; Kumar, S. The Mechanical Rigidity of the Extracellular Matrix Regulates the Structure, Motility, and Proliferation of Glioma Cells. *Cancer Res.* **2009**, *69*, 4167−4174.
(31) Heddleston, J. M.; Li, Z.; McLendon, R. E.; Hjelmeland, A. B.; Rich, J. N. The Hypoxic Microenvironment Maintains Glioblastoma Stem Cells and Promotes Reprogramming towards a Cancer Stem Cell Phenotype. *Cell Cycle* **2009**, *8*, 3274−3284.
(32) Liu, J.; Tan, Y.; Zhang, H.; Zhang, Y.; Xu, P.; Chen, J.; Poh, Y.-C.; Tang, K.; Wang, N.; Huang, B. Soft Fibrin Gels Promote Selection and Growth of Tumorigenic Cells. *Nat. Mater.* **2012**, *11*, 734−741.
(33) Wong, S. Y.; Ulrich, T. A.; Deleyrolle, L. P.; MacKay, J. L.; Lin, J.-M. G.; Martuscello, R. T.; Jundi, M. A.; Reynolds, B. A.; Kumar, S. Constitutive Activation of Myosin-Dependent Contractility Sensitizes Glioma Tumor-Initiating Cells to Mechanical Inputs and Reduces Tissue Invasion. *Cancer Res.* **2015**, *75*, 1113−1122.
(34) Sunyer, R.; Jin, A. J.; Nossal, R.; Sackett, D. L. Fabrication of Hydrogels with Steep Stiffness Gradients for Studying Cell Mechanical Response. *PLoS One* **2012**, *7*, No. e46107.
(35) Lam, C. R. I.; Wong, H. K.; Nai, S.; Chua, C. K.; Tan, N. S.; Tan, L. P. A 3D Biomimetic Model of Tissue Stiffness Interface for Cancer Drug Testing. *Mol. Pharm.* **2014**, *11*, 2016−2021.
(36) Kuo, C.-H. R.; Xian, J.; Brenton, J. D.; Franze, K.; Sivaniah, E. Complex Stiffness Gradient Substrates for Studying Mechanotactic Cell Migration. *Adv. Mater.* **2012**, *24*, 6059−6064.
(37) Koser, D. E.; Thompson, A. J.; Foster, S. K.; Dwivedy, A.; Pillai, E. K.; Sheridan, G. K.; Svoboda, H.; Viana, M.; Costa, L. d. F.; Guck, J.; Holt, C. E.; Franze, K. Mechanosensing Is Critical for Axon Growth in the Developing Brain. *Nat. Neurosci.* **2016**, *19*, 1592−1598.
(38) Tse, J. R.; Engler, A. J. Stiffness Gradients Mimicking in Vivo Tissue Variation Regulate Mesenchymal Stem Cell Fate. *PLoS One* **2011**, *6*, No. e15978.
(39) Hadden, W. J.; Young, J. L.; Holle, A. W.; McFetridge, M. L.; Kim, D. Y.; Wijesinghe, P.; Taylor-Weiner, H.; Wen, J. H.; Lee, A. R.; Bieback, K.; Vo, B.-N.; Sampson, D. D.; Kennedy, B. F.; Spatz, J. P.; Engler, A. J.; Choi, Y. S. Stem Cell Migration and Mechanotransduction on Linear Stiffness Gradient Hydrogels. *Proc. Natl. Acad. Sci. U.S.A.* **2017**, *114*, 5647−5652.
(40) Lee, J.; Abdeen, A. A.; Wycislo, K. L.; Fan, T. M.; Kilian, K. A. Interfacial Geometry Dictates Cancer Cell Tumorigenicity. *Nat. Mater.* **2016**, *15*, 856−862.
(41) Lee, J.; Abdeen, A. A.; Hedhli, J.; Wycislo, K. L.; Dobrucki, I. T.; Fan, T. M.; Dobrucki, L. W.; Kilian, K. A. Melanoma Topology Reveals a Stem-like Phenotype That Promotes Angiogenesis. *Sci. Adv.* **2017**, *3*, No. e1701350.
(42) Lee, J.; Molley, T. G.; Seward, C. H.; Abdeen, A. A.; Zhang, H.; Wang, X.; Gandhi, H.; Yang, J.-L.; Gaus, K.; Kilian, K. A. Geometric Regulation of Histone State Directs Melanoma Reprogramming. *Commun. Biol.* **2020**, *3*, 341.
(43) Lee, J.; Abdeen, A. A.; Huang, T. H.; Kilian, K. A. Controlling Cell Geometry on Substrates of Variable Stiffness Can Tune the Degree of Osteogenesis in Human Mesenchymal Stem Cells. *J. Mech. Behav. Biomed. Mater.* **2014**, *38*, 209−218.

https://dx.doi.org/10.1021/acsabm.0c01263
ACS Appl. Bio Mater. XXXX, XXX, XXX−XXX

(44) Abdeen, A. A.; Lee, J.; Bharadwaj, N. A.; Ewoldt, R. H.; Kilian, K. A. Temporal Modulation of Stem Cell Activity Using Magneto-active Hydrogels. *Adv. Healthcare Mater.* **2016**, *5*, 2536−2544.
(45) Zhang, D.; Lee, J.; Sun, M. B.; Pei, Y.; Chu, J.; Gillette, M. U.; Fan, T. M.; Kilian, K. A. Combinatorial Discovery of Defined Substrates That Promote a Stem Cell State in Malignant Melanoma. *ACS Cent. Sci.* **2017**, *3*, 381−393.
(46) Oudin, M. J.; Eaver, V. M. Physical and Chemical Gradients in the Tumor Microenvironment Regulate Tumor Cell Invasion, Migration, and Metastasis. *Cold Spring Harbor Symp. Quant. Biol.* **2016**, *81*, 189−205.
(47) Laklai, H.; Miroshnikova, Y. A.; Pickup, M. W.; Collisson, E. A.; Kim, G. E.; Barrett, A. S.; Hill, R. C.; Lakins, J. N.; Schlaepfer, D. D.; Mouw, J. K.; LeBleu, V. S.; Roy, N.; Novitskiy, S. V.; Johansen, J. S.; Poli, V.; Kalluri, R.; Iacobuzio-Donahue, C. A.; Wood, L. D.; Hebrok, M.; Hansen, K.; Moses, H. L.; Weaver, V. M. Genotype Tunes Pancreatic Ductal Adenocarcinoma Tissue Tension to Induce Matricellular Fibrosis and Tumor Progression. *Nat. Med.* **2016**, *22*, 497−505.
(48) Petrie, R. J.; Doyle, A. D.; Yamada, K. M. Random versus Directionally Persistent Cell Migration. *Nat. Rev. Mol. Cell Biol.* **2009**, *10*, 538−549.
(49) Levental, K. R.; Yu, H.; Kass, L.; Lakins, J. N.; Egeblad, M.; Erler, J. T.; Fong, S. F. T.; Csiszar, K.; Giaccia, A.; Weninger, W.; Yamauchi, M.; Gasser, D. L.; Weaver, V. M. Matrix Crosslinking Forces Tumor Progression by Enhancing Integrin Signaling. *Cell* **2009**, *139*, 891−906.
(50) Joshi, B.; Strugnell, S. S.; Goetz, J. G.; Kojic, L. D.; Cox, M. E.; Griffith, O. L.; Chan, S. K.; Jones, S. J.; Leung, S.-P.; Masoudi, H.; Leung, S.; Wiseman, S. M.; Nabi, I. R. Phosphorylated Caveolin-1 Regulates Rho/ROCK-Dependent Focal Adhesion Dynamics and Tumor Cell Migration and Invasion. *Cancer Res.* **2008**, *68*, 8210−8220.
(51) Zhang, X.; Lin, M.; Van Golen, K. L.; Yoshioka, K.; Itoh, K.; Yee, D. Multiple Signaling Pathways Are Activated during Insulin-like Growth Factor-I (IGF-I) Stimulated Breast Cancer Cell Migration. *Breast Cancer Res. Treat.* **2005**, *93*, 159−168.
(52) Sampath, K. T. *Bone Morphogenetic Proteins: Systems Biology Regulators*; Springer, 2017.
(53) Pal, A.; Huang, W.; Li, X.; Toy, K. A.; Nikolovska-Coleska, Z.; Kleer, C. G. CCN6 Modulates BMP Signaling via the Smad-Independent TAK1/P38 Pathway, Acting to Suppress Metastasis of Breast Cancer. *Cancer Res.* **2012**, *72*, 4818−4828.
(54) Garulli, C.; Kalogris, C.; Pietrella, L.; Bartolacci, C.; Andreani, C.; Falconi, M.; Marchini, C.; Amici, A. Dorsomorphin Reverses the Mesenchymal Phenotype of Breast Cancer Initiating Cells by Inhibition of Bone Morphogenetic Protein Signaling. *Cell. Signalling* **2014**, *26*, 352−362.
(55) Uchino, M.; Kojima, H.; Wada, K.; Imada, M.; Onoda, F.; Satofuka, H.; Utsugi, T.; Murakami, Y. Nuclear β-catenin and CD44 upregulation characterize invasive cell populations in non-aggressive MCF-7 breast cancer cells. *BMC Cancer* **2010**, *10*, 414.

https://dx.doi.org/10.1021/acsabm.0c01263
ACS Appl. Bio Mater. XXXX, XXX, XXX−XXX